bution and properties of the nanocrystals obtained by this method. Two potential applications of nanocrystals have been demonstrated, one dealing with perpendicular magnetization of γ-Fe_2O_3 films and the other with nanolithography using Au nanocrystals.

1. Schmid, G., *Clusters and Colloids: From Theory to Applications*, Wiley-VCH, Weinheim, 1994.
2. Fendler, J. H., *Nanoparticles and Nanostructured Films Preparation, Characterization and Applications*, Wiley-VCH, Weinheim, 1998.
3. Rao, C. N. R., Kulkarni, G. U., Thomas, P. J. and Edwards, P. P., Size-dependent chemistry: Properties of nanocrystals. *Chem. Eur. J.*, 2002, **8**, 29–35.
4. Trindade, T., O'Brien, P. and Pickett, N. L., Nanocrystalline semiconductors: synthesis, properties and perspectives. *Chem. Mater.*, 2001, **13**, 3843–3558; Esteves., A. C. C. and Trindade, T., Synthetic studies on II/VI semiconductor quantum dots. *Curr. Opinion Solid State Mater. Sci.*, 2002, **6**, 347–353.
5. Green, M., Solution routes to III–V semiconductor quantum dots. *Curr. Opinion Solid State Mater. Sci.*, 2002, **6**, 355–363.
6. Pileni, M.-P., The role of soft colloidal templates in controlling the size and shape of inorganic nanocrystals. *Nature Mater.*, 2003, **2**, 145–150.
7. Brust, M., Bethell, D., Schiffrin, D. J. and Kiely, C. J., Novel gold-dithiol nano-networks with non-metallic electronic properties. *Adv. Mater.*, 1995, **7**, 795–797.
8. Rockenberger, J., Scher, E. J. and Alivisatos, A. P., A new non-hydrolytic single precursor approach to surfactant-capped nanocrystals of transition metal oxides. *J. Am. Chem. Soc.*, 1999, **121**, 11595–11596.
9. Murray, C. B., Norris, D. J. and Bawendi, M. G., Synthesis and characterization of nearly monodisperse CdE (E = sulfur, selenium, tellurium) semiconductor nanocrystallites. *J. Am. Chem. Soc.*, 1993, **115**, 8706–8715.
10. Sarathy, K. V., Kulkarni, G. U. and Rao, C. N. R., A novel method of preparing thiol-derivarised nanoparticles of gold, platinum and silver forming superstructures. *J. Chem. Soc., Chem. Commun.*, 1997, 537–538.
11. Duff, D. G., Baiker, A. and Edwards, P. P., A new hydrosol of gold clusters. 1. Formation and particle size variation. *Langmuir*, 1993, **9**, 2301–2309.
12. Duff, D. G., Baiker, A., Gameson, I. and Edwards, P. P., A new hydrosol of gold structures. 2. A comparison of some different measurement techniques. *Langmuir*, 1993, **9**, 2310–2317.
13. Zeng, H., Li, J., Liu, J. P., Wang, Z. L. and Sun, S., Exchange-coupled nanocomposite magnets by nanoparticle self-assembly. *Nature*, 2002, **420**, 395–398; Sun, S., Murray, C. B., Weller, D., Folks, L. and Moser, A., Monodisperse FePt nanoparticles and ferromagnetic FePt nanocrystal superlattices. *Science*, 2000, **287**, 1989–1992; Ngo, A. T. and Pileni, M. P., Assemblies of ferrite nanocrystals: Partial orientation of the easy magnetic axes. *J. Phys. Chem. B*, 2001, **105**, 53–58.
14. Demers, L. M. and Mirkin, C. A., Combinatorial templates generated by dip-pen nanolithography for the formation of two-dimensional particle arrays. *Angew. Chem., Int. Ed. Engl.*, 2001, **40**, 3069–3071.

ACKNOWLEDGEMENTS. We thank the DRDO and the Department of Science and Technology for support. U.K.G. thanks CSIR for a senior research fellowship.

Received 8 September 2003

Structural and dynamical consequences on various high-pressure phase transitions in laser host fluoroscheelites $LiYF_4$ and $LiYbF_4$*

A. Sen, S. L. Chaplot† and R. Mittal

Solid State Physics Division, Bhabha Atomic Research Centre, Trombay, Mumbai 400 085, India

Computer simulations of pressure-induced phase transitions in $LiYF_4$ and $LiYbF_4$ have been carried out using complementary techniques of molecular dynamics (MD) and lattice dynamics. The MD simulations at a constant temperature of 300 K with increasing pressure reveal structural changes at around 5 and 15 GPa and the crystallographic space groups of the new structures. The lattice dynamics calculations are then conveniently used to derive the vibrational spectra and the free energies and its consequences on the thermodynamic stability of the new phases.

IN recent years, lithium rare earth fluoroscheelites such as $LiYF_4$ and $LiYbF_4$ have been studied extensively[1–16] with a view to better-understand their thermal and optical properties that are exhibited upon doping with trivalent rare-earth ions (e.g. Nd^{3+}, Ho^{3+}, Eu^{3+}, etc.) in a wide range (UV–IR) of highly efficient lasing actions. Both $LiYF_4$ and $LiYbF_4$ crystallize under ambient conditions in the tetragonal scheelite structure (space group: $I4_1/a$, $Z = 4$), with two molecules in the unit cell[6]. Although isostructural with oxoscheelites (viz. $CaWO_4$), these compounds have different pressure responses compared to that of the former, making them worthy for further study, especially in areas of high-pressure phase transitions.

As we know, pressure reduces the volume of a substance, thereby causing significant changes in its electronic and vibronic states, chemical bonding and atomic packing. Hence, investigations of pressure-dependent optic and thermodynamic properties often yield invaluable information on many properties of materials at high pressures. Pressure-dependent Raman study by Saratopoulou *et al.*[10] has already pointed out an abrupt change of slope in the frequency versus pressure diagrams of phonon modes at 7 GPa, signifying the onset of structural instabilities in $LiYF_4$ with increase in pressure. This observation was supported by our previous lattice-dynamical work[11], where we have shown the splitting of B_g/E_g Raman lines in the vicinity of 350 and 400 cm^{-1}. We further attribute the initiation of discontinuities in the Raman spectra of $LiYF_4$ to the softening of transverse acoustic phonon modes in the direction of dynamical insta-

*Dedicated to Prof. S. Ramaseshan on his 80th birthday.

†For correspondence. (e-mail: chaplot@magnum.barc.ernet.in)

bility[11]. This fact that leads to a pressure-induced structural phase transition was experimentally observed by Grzechnik *et al.*[12], while carrying out the angle-dispersive high-pressure X-ray powder diffraction study. Recent room-temperature luminescence measurements on Eu^{3+}-doped $LiYF_4$ by Manjon *et al.*[13] have also indicated a subtle anomaly in the structural parameters of the scheelite phase of $LiYF_4$ near 10.3 GPa, associated with the lowering of crystal symmetry.

Numerous contemporary studies, including that of Grzechnik *et al.*[12] demonstrate that while oxoscheelites generally transform under compression within 11 GPa from the tetragonal scheelite structure to the monoclinic wolframite one (space group: P2/c, $Z = 2$), fluoroscheelites on the other hand, make it somewhat different by transforming themselves from the identical structure to the monoclinic fergusonite-like polymorph (space group: C2/c, $Z = 4$ above 300 K and space group: $P2_1/c$, $Z = 4$ at 0–300 K) under similar pressure conditions. However, reversibility to the initial structure after a small hysteresis has been observed to take place in both kinds of scheelites, suggesting that this kind of phase transition is nearly of second-order. In order to understand the transformation mechanisms of such pressure-driven transitions, one has to study the pressure effects on the local atomic structure. Hence, we have carried out molecular dynamics (MD) simulations[14] on $LiYF_4$ as well as $LiYbF_4$ over a wide range of pressure (0–100 GPa) and compared our results with several experimental findings as mentioned above. In this process, we are also able to analyse the hitherto unidentified second-phase transition, which comes out to be of the first-order kind.

In this communication, we restrict ourselves mainly to analysing various high-pressure phases derived from either experiments or MD simulations. The aim is essentially to have an overall idea of what may be the structural as well as the dynamical consequences on various high-pressure phase transitions in $LiYF_4$ and $LiYbF_4$. To accomplish this we pursue extensive lattice-dynamical calculations separately for the two high-pressure phases and analyse the results in view of our earlier observations[11,15].

The well-established technique of lattice-dynamics, which was described in detail by Born and Huang[16] way back in 1954, essentially involves setting up a dynamical matrix of force constants followed by its subsequent diagonalization for obtaining phonon frequencies (pertaining to different types of acoustic and optic modes) along with polarization vectors. We carry out extensive lattice-dynamical calculations for the present fluoroscheelite system under ambient conditions by developing a transferable rigid ion model[15] in the quasi-harmonic approximations. This model[15] validated by several experimental data[1–10], provides a sensitive test for the interatomic potential relevant to the system under study. Broadly speaking, our model potential function consists of a string of three energy terms, viz. Coulombic, Born–Mayer-type (repulsive) and van der Waals-type (weak attractive) interactions. The adjustable parameters used in the model, which are only five in number, are chosen to satisfy both static and dynamic equilibrium. Computations of phonon frequencies are performed using DISPR[17], developed at Trombay. The advantage with such quasi-harmonic lattice-dynamics (QLD) lies in its ability to calculate free energies and derived properties (e.g. entropy and heat capacity) with high precision. However, QLD can be best exploited up to a temperature beyond which the anharmonicity of lattice vibrations becomes too large. It is simply because at very high temperatures, the dynamics may not be described to the full in terms of phonons alone. Rather, other related phenomena such as diffusion and molecular reorientation turn out to be significant. In such situations, the MD technique[18,19] in simulating the time evolution of structure under the effect of pressure as well as temperature is useful.

Given initial positions and velocities, the evolution of a system is, in principle, correctly determined[20,21] through MD simulations to enhance our knowledge on various macroscopic properties of interest. One of the main strengths of the MD method is that it can deal with fast, non-equilibrium processes also. Classical MD simulations[19], which make use of a suitable interatomic potential, involve integrations of the equations of motion to obtain atomic trajectories. In the present case, the equations of motion are integrated with a time step of 1 fs for periodic macro cells of 768 atoms. Since the important correlations involved are essentially of short range (< 1 nm), this cell width is considered to be quite satisfactory. The long-range two-body Coulomb interactions are integrated by the Ewald technique, while the other potential terms, owing to their short-range order, are directly summed up over all the pairs (up to 7 Å separation). Periodic boundary conditions are applied across the macro cell in order to get rid of unwanted surface effects. We monitored the volume, temperature and also atomic trajectories during the course of our MD simulation.

Under the effect of pressure, the ambient scheelite phase of both the compounds $LiYF_4$ and $LiYbF_4$ exhibits appreciable changes in structure[12,14]. We took into account the dynamical contributions to the equation of state (EOS) in MD simulations[14]. As we look at the EOS (Figure 1), we realize that the bifurcations in the lattice parameters around 5 GPa, symbolizing the onset of new phases, are mainly the outcome of the lattice distortions under compression. From our MD simulations, the monoclinic angle of distortion (given by β) for the second phase gradually increases to 98° for $LiYF_4$ as against the experimentally determined[12] value of 95.3°. Going by usual conventions, this phase change from tetragonal to monoclinic calls for a relabelling of unit cell axes from *a*, *b*, *c* to *c*, *a*, *b*, respectively. As evident from Figure 1, a discontinuity in the lattice parameters is found to occur at a pressure above 15 GPa, implying a first-order kind of phase

transition. Further, analysis suggests a volume drop of nearly 6% in $LiYF_4$ and 7% in $LiYbF_4$ during this pressure-induced phase transformation.

Our simulation results based on a semi-empirical potential show that the lithium rare-earth fluoroscheelites undergo two high-pressure transitions, one within (or near) 10 GPa and the other within 20 GPa, in agreement with the high-pressure X-ray diffraction study[12]. Further, with the aid of complementary lattice-dynamical calculations, we establish that the dynamically stable, first high-pressure phase of $LiYF_4$ as well as $LiYbF_4$ has an energy-minimized structure pertaining to the space group $P2_1/c$ ($Z = 40$) in the low-temperature region (0–300 K), and C2/c ($Z = 4$) above 300 K. Our previous work[14] has discussed this in detail. In fact, the atomic shifts on going from $P2_1/c$ to C2/c have been found to be small (below 0.2 Å), which may not be well-differentiated during X-ray diffraction studies at such high pressures. However, from the atomic arrangements, we come to know that the second stable phase of the fluoroscheelites mimics a fergusonite-like structure. With further increase in pressure, another new high-pressure phase appears that has a high β value (~ 108°). This new configuration, which is also monoclinic in nature ($P2_1/c$, $Z = 4$), remains stable even at 100 GPa. Figure 2 shows how atomic positions of fluoroscheelites shift on going from one phase to the other.

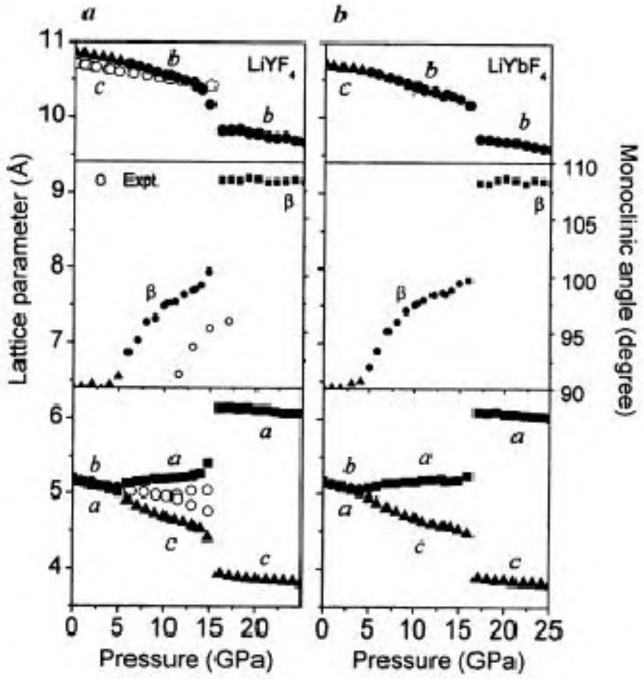

Figure 1. Pressure variation in lattice parameters (*a*, *b*, *c*: left scale, β: right scale) of the ambient scheelite structure of $LiYF_4$ (***a***) and $LiYbF_4$ (***b***) upon compression. Open symbols depict the high-pressure X-ray diffraction data of Grzechnik *et al.*[12] while closed ones represent our simulated results.

We have shown[11] that dynamical instability arises in fluoroscheelites because of the softening of some transverse acoustic phonon modes (Figure 3 *c*). The soft phonon provides one of the mechanisms by which crystal structures transform upon compression, to a lower symmetry phase.

From the group theoretical analysis for the ambient scheelite phase, we find that 36 zone-centre phonon modes are distributed among various irreducible representations[11,15]. The doubly degenerate modes of E_g and E_u symmetry are plotted as a function of pressure in Figure 3.

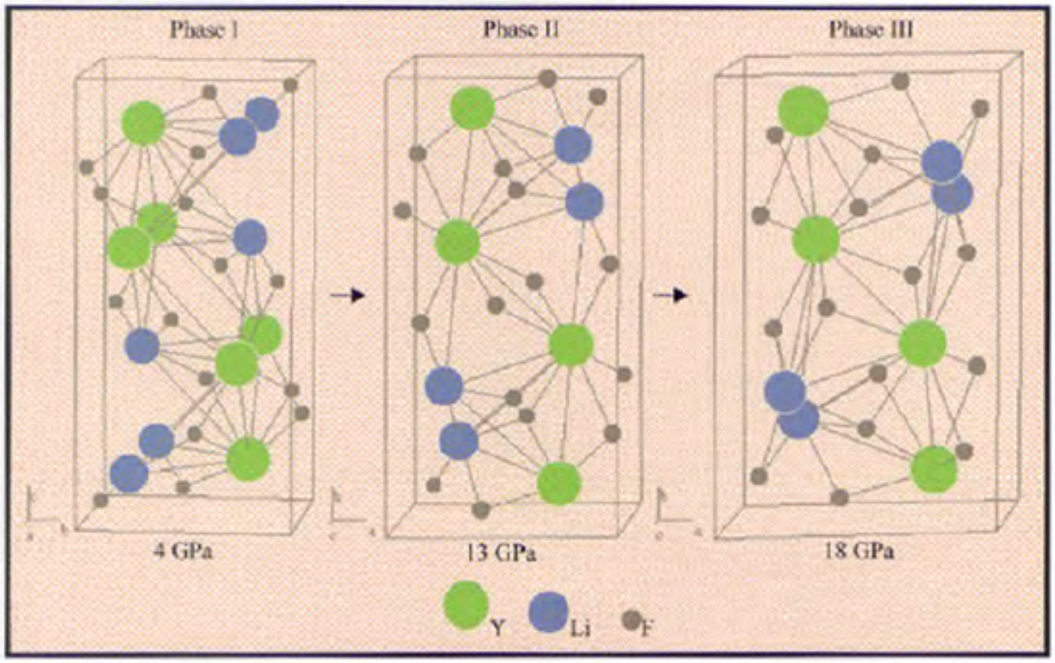

Figure 2. Simulated structures in scheelite (***a***), fergusonite-like (***b***) and new monoclinic (***c***) phases of $LiYF_4$ at 4, 13 and 18 GPa respectively.

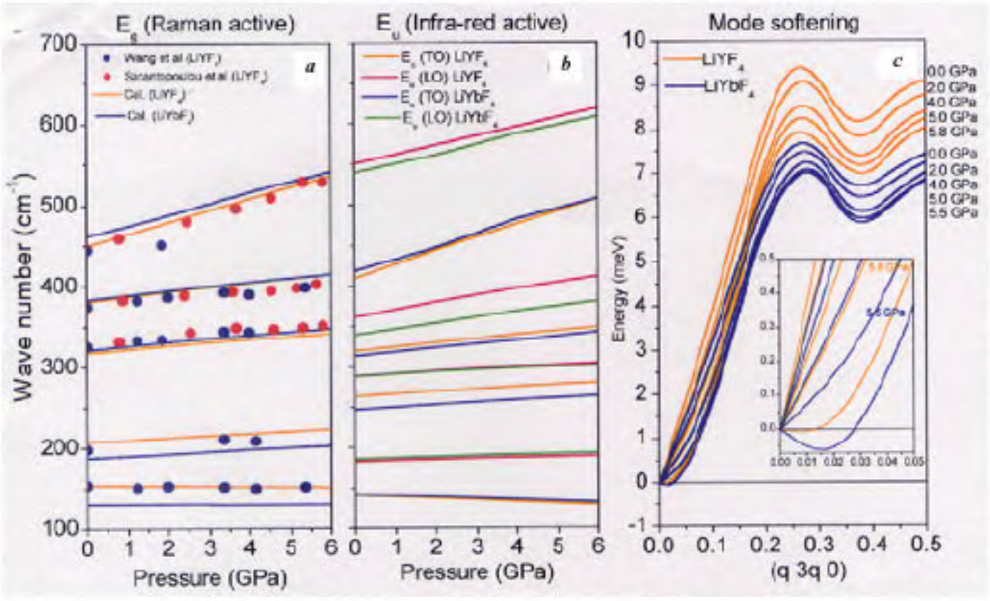

Figure 3. Pressure variation of (***a***) Raman active E_g modes; (***b***) infrared active E_u modes and (***c***) transverse acoustic phonon branch (along the direction of dynamical instability) in $LiYF_4$ and $LiYbF_4$. Circles depict the experimental data[10,22]. Lines represent the lattice-dynamical calculations for $LiYF_4$ and $LiYbF_4$.

A fair degree of parity is observed between experiments[10,22] and our lattice-dynamical calculations. However, we have not been able to compare the degenerate infrared modes due to lack of measured data. As seen from Figure 3, the low-lying Raman frequencies of $LiYF_4$ and $LiYbF_4$ exhibit shifts in the E_g modes, which supports the observations of Sarantopoulou *et al.*[10] that the low frequency modes of E_g symmetry are sensitive to rare-earth substitution. For the E_u modes, we come across a different situation. Both the longitudinal optic (LO) and transverse optic (TO) vibrations in the similar low-frequency range display almost similar behaviour for $LiYF_4$ and $LiYbF_4$ upon compression. Higher vibrational modes show larger variations with pressure in the fluoroscheelite system, before any phase change occurs.

The relative stability of various high-pressure phases at a finite temperature can be obtained if the phonon spectra in all the different phases are also evaluated. To have an overview of the range and extent of various phonon modes in the three phases (at 4, 13 and 18 GPa, respectively), we integrate over all the phonons with an energy resolution of 1 meV at each wavevector on a $4 \times 4 \times 4$ mesh, within the irreducible Brillouin zone. Figure 4 shows that the energy distribution extends by nearly 10% on application of pressure. We further notice that considerable shift in the phonon spectra occurs mainly after 60 meV, contribution of the lightest atom Li is quite significant to make this shift happen. From our earlier work[11], we know that the effect of pressure on rare-earth substitution is quite negligible.

The stability of a crystalline phase is largely determined by the minimization of the Gibbs free-energy ($= U + PV - TS$), which includes the vibrational energy

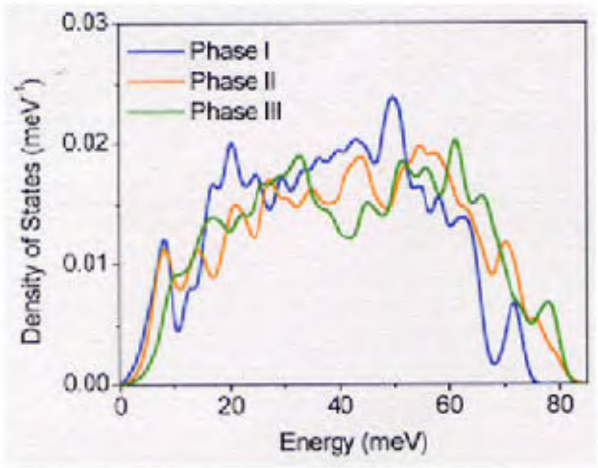

Figure 4. Comparison of phonon density of states as a function of pressure in the three phases of $LiYF_4$ at 4, 13 and 18 GPa respectively.

and vibrational entropy[23]. Hence, it would be quite interesting if we can compare the phase-wise free-energy diagrams at one shot. We calculated free energies at different pressures in the three phases. The result is plotted in Figure 5. The free-energy plot of the phase I joins smoothly at 5 GPa to that of phase II, which is consistent with the nature of (second-order) phase transition. Beyond 8 GPa, phase III has a lower free-energy that indicates greater stability of this phase and a first-order phase transition from phase II to phase III. The transition pressure in MD simulation, while increasing pressures, is higher than 8 GPa due to hysteresis. We note that the greater stability of phase III at high pressures arises primarily due to its lower volume, while the vibrational energy is also lower and the entropy is higher in phase III providing an additional stability.

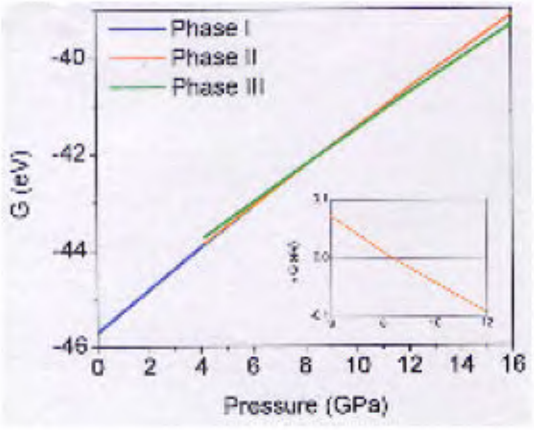

Figure 5. Comparison of Gibbs free-energy per formula unit of $LiYF_4$ as a function of pressure in the three phases respectively, as obtained from the lattice-dynamical calculations. (Inset) Variation in Gibbs energy difference (δG) with pressure which gives a qualitative impression of the first-order phase transition that takes place on going from phase II to a more stable phase III.

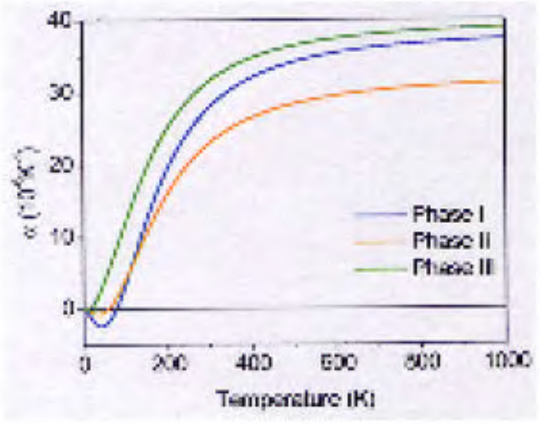

Figure 6. An overview of volume thermal expansion with varying temperature in the three phases of $LiYF_4$ at 4, 13 and 18 GPa respectively.

The effect of pressure on the volume coefficient of thermal expansion (α), usually defined as the fractional change in cell volume with temperature, can be studied through mode Grüneisen parameters,

$$\Gamma_i = -\frac{\partial \ln \omega_i}{\partial \ln V},$$

in the entire Brillouin zone, for each of the three phases. Figure 6 demonstrates the variation of α. In the quasi-harmonic approximation, each phonon mode of energy E_i contributes to the thermal expansion by way of,

$$\left(\frac{1}{BV}\right)\Gamma_i C_{V_i},$$

where B is the bulk modulus associated with a particular phase, V the corresponding unit cell volume, and C_{Vi} the specific heat (at constant volume) contribution of the ith mode. This procedure suits well the present fluoro-scheelite system because explicit anharmonicity, which arises mainly out of thermal amplitudes is not significant compared to the implicit effect that involves phonon frequency change with volume to be obtained from Γ_i. As Figure 6 depicts, the ambient as well as the initial high-pressure phase of $LiYF_4$ have negative thermal expansion in low-temperature limit (below 100 K). This is so because the Grüneisen gamma has large negative values for phonons below 8 meV at these two phases. However, the third phase has no such anomaly, again because it has all positive gammas for phonons of all energies.

Results of this work show that even a simple model potential can be successfully exploited through classical simulations in understanding many important physical properties of relevant solid materials at high pressures. Complementary lattice dynamics calculations may reveal the presence of soft vibrational modes that may be related to phase transformations. Further, the relative stability of various crystalline phases is shown through a comparison of their respective Gibbs free energies with contributions from both the structure and the vibrations.

1. Millar, S. A., Rasty, H. E. and Caspers, H. H., *J. Chem. Phys.*, 1970, **52**, 4172.
2. Blanchfield, P. and Saunders, G. A., *J. Phys. C*, 1979, **12**, 4673.
3. Blanchfield, P., Tu Hailing, Miller, A. J., Saunders, G. A. and Chapman, B., *J. Phys. C*, 1983, **20**, 3851.
4. Misiak, L., Mikolajczak, P. and Subotowicz, M., *Phys. Status Solidi A*, 1986, **97**, 353.
5. Schultheiss, E., Scharmann, A. and Schwabe, D., *Phys. Status Solidi B*, 1986, **138**, 465.
6. Garcia, E. and Ryan, R. R., *Acta Crysallogr., Sect. C*, 1993, **49**, 2053.
7. Zhang, X. X., Schulte, A. and Chai, B. H. T., *Solid State Commun.*, 1994, **89**, 181.
8. Salaün, S., Fornoni, M. T., Bulou, A., Rousseau, M., Simon, P. and Gesland, J. Y., *J. Phys.: Condens. Matter*, 1997, **9**, 6941.
9. Salaün, S., Bulou, A., Rousseau, M., Hennion, B. and Gesland, J. Y., *J. Phys.: Condens. Matter*, 1997, **9**, 6957.
10. Sarantopoulou, E., Raptis, Y. S., Zouboulis, E. and Raptis, C., *Phys. Rev. B*, 1999, **59**, 4154.
11. Sen, A., Chaplot, S. L. and Mittal, R., *J. Phys.: Condens. Matter*, 2002, **14**, 975.
12. Grzechnik, A., Syassen, K., Loa, I., Hanfland, M. and Gesland, J. Y., *Phys. Rev. B*, 2002, **65**, 104102.
13. Manjon, F. J., Jandl, S., Syassen, K. and Gesland, J. Y., *Phys. Rev. B*, 2001, **64**, 235108.
14. Sen, A., Chaplot, S. L. and Mittal, R., *Phys. Rev. B*, 2003, **68**, (in press).
15. Sen, A., Chaplot, S. L. and Mittal, R., *Phys. Rev. B*, 2001, **64**, 024304.
16. Born, M. and Huang, K., *Dynamical Theory of Crystal Lattices*, Oxford, Clarendon, 1954; Venkataraman, G., Feldkamp, L. and Sahni, V. C., *Dynamics of Perfect Crystals*, MIT Press, Cambridge, 1975.
17. Chaplot, S. L., External Report, BARC-972, 1978; 1992, unpublished.
18. Rahman, A., *Phys. Rev. A*, 1964, **136**, 105.
19. Parrinello, M. and Rahman, A., *Phys. Rev. Lett.*, 1980, **45**, 1196.
20. Chaplot, S. L. and Rao, K. R., *Phys. Rev. B*, 1987, **35**, 9771.
21. Chaplot, S. L. and Sikka, S. K., *Phys. Rev. B*, 1993, **47**, 5710.
22. Wang, Q. A., Bulou, A. and Gesland, J. Y., 2001, private commun.
23. Chaplot, S. L., *Phys. Rev. B*, 1987, **36**, 8471.

ACKNOWLEDGMENTS. A.S. would like to express his earnest gratitude towards the Council of Scientific and Industrial Research (CSIR), New Delhi, for rendering necessary financial assistance during the work.

Received 3 September 2003